

## Search for $D^0 - \bar{D}^0$ mixing using semileptonic decays at Belle

U. Bitenc,<sup>12</sup> K. Abe,<sup>7</sup> K. Abe,<sup>40</sup> I. Adachi,<sup>7</sup> H. Aihara,<sup>42</sup> Y. Asano,<sup>46</sup> T. Aushev,<sup>11</sup> S. Bahinipati,<sup>4</sup> S. Banerjee,<sup>38</sup>  
 E. Barberio,<sup>18</sup> M. Barbero,<sup>6</sup> I. Bedny,<sup>1</sup> I. Bizjak,<sup>12</sup> S. Blyth,<sup>21</sup> A. Bondar,<sup>1</sup> A. Bozek,<sup>24</sup> M. Bračko,<sup>7, 17, 12</sup>  
 J. Brodzicka,<sup>24</sup> T. E. Browder,<sup>6</sup> Y. Chao,<sup>23</sup> A. Chen,<sup>21</sup> W. T. Chen,<sup>21</sup> B. G. Cheon,<sup>3</sup> R. Chistov,<sup>11</sup> Y. Choi,<sup>36</sup>  
 A. Chuvikov,<sup>32</sup> S. Cole,<sup>37</sup> J. Dalseno,<sup>18</sup> M. Danilov,<sup>11</sup> M. Dash,<sup>47</sup> L. Y. Dong,<sup>9</sup> J. Dragic,<sup>7</sup> A. Drutskoy,<sup>4</sup>  
 S. Eidelman,<sup>1</sup> Y. Enari,<sup>19</sup> S. Fratina,<sup>12</sup> N. Gabyshev,<sup>1</sup> T. Gershon,<sup>7</sup> A. Go,<sup>21</sup> G. Gokhroo,<sup>38</sup> B. Golob,<sup>16, 12</sup>  
 A. Gorišek,<sup>12</sup> J. Haba,<sup>7</sup> K. Hayasaka,<sup>19</sup> H. Hayashii,<sup>20</sup> M. Hazumi,<sup>7</sup> T. Hokuue,<sup>19</sup> Y. Hoshi,<sup>40</sup> S. Hou,<sup>21</sup>  
 W.-S. Hou,<sup>23</sup> T. Iijima,<sup>19</sup> K. Ikado,<sup>19</sup> A. Imoto,<sup>20</sup> A. Ishikawa,<sup>7</sup> R. Itoh,<sup>7</sup> M. Iwasaki,<sup>42</sup> Y. Iwasaki,<sup>7</sup> J. H. Kang,<sup>48</sup>  
 J. S. Kang,<sup>14</sup> P. Kapusta,<sup>24</sup> S. U. Kataoka,<sup>20</sup> N. Katayama,<sup>7</sup> H. Kawai,<sup>2</sup> T. Kawasaki,<sup>26</sup> H. R. Khan,<sup>43</sup> H. Kichimi,<sup>7</sup>  
 J. H. Kim,<sup>36</sup> S. M. Kim,<sup>36</sup> K. Kinoshita,<sup>4</sup> S. Korpar,<sup>17, 12</sup> P. Križan,<sup>16, 12</sup> P. Krokovny,<sup>1</sup> C. C. Kuo,<sup>21</sup> Y.-J. Kwon,<sup>48</sup>  
 J. S. Lange,<sup>5</sup> G. Leder,<sup>10</sup> S. E. Lee,<sup>34</sup> T. Lesiak,<sup>24</sup> J. Li,<sup>33</sup> D. Liventsev,<sup>11</sup> F. Mandl,<sup>10</sup> T. Matsumoto,<sup>44</sup>  
 A. Matyja,<sup>24</sup> W. Mitaroff,<sup>10</sup> H. Miyake,<sup>29</sup> H. Miyata,<sup>26</sup> Y. Miyazaki,<sup>19</sup> R. Mizuk,<sup>11</sup> D. Mohapatra,<sup>47</sup>  
 G. R. Moloney,<sup>18</sup> T. Nagamine,<sup>41</sup> Y. Nagasaka,<sup>8</sup> E. Nakano,<sup>28</sup> Z. Natkaniec,<sup>24</sup> S. Nishida,<sup>7</sup> O. Nitoh,<sup>45</sup>  
 T. Nozaki,<sup>7</sup> S. Ogawa,<sup>39</sup> T. Ohshima,<sup>19</sup> T. Okabe,<sup>19</sup> S. Okuno,<sup>13</sup> S. L. Olsen,<sup>6</sup> Y. Onuki,<sup>26</sup> W. Ostrowicz,<sup>24</sup>  
 P. Pakhlov,<sup>11</sup> H. Palka,<sup>24</sup> C. W. Park,<sup>36</sup> N. Parslow,<sup>37</sup> R. Pestotnik,<sup>12</sup> L. E. Piilonen,<sup>47</sup> Y. Sakai,<sup>7</sup>  
 N. Satoyama,<sup>35</sup> K. Sayeed,<sup>4</sup> T. Schietinger,<sup>15</sup> O. Schneider,<sup>15</sup> A. J. Schwartz,<sup>4</sup> M. E. Sevier,<sup>18</sup> H. Shibuya,<sup>39</sup>  
 B. Shwartz,<sup>1</sup> V. Sidorov,<sup>1</sup> A. Somov,<sup>4</sup> N. Soni,<sup>30</sup> S. Stanič,<sup>27</sup> M. Starič,<sup>12</sup> K. Sumisawa,<sup>29</sup> T. Sumiyoshi,<sup>44</sup>  
 F. Takasaki,<sup>7</sup> K. Tamai,<sup>7</sup> N. Tamura,<sup>26</sup> M. Tanaka,<sup>7</sup> Y. Teramoto,<sup>28</sup> X. C. Tian,<sup>31</sup> T. Tsuboyama,<sup>7</sup>  
 T. Tsukamoto,<sup>7</sup> S. Uehara,<sup>7</sup> T. Uglov,<sup>11</sup> Y. Unno,<sup>7</sup> S. Uno,<sup>7</sup> P. Urquijo,<sup>18</sup> G. Varner,<sup>6</sup> S. Villa,<sup>15</sup> C. H. Wang,<sup>22</sup>  
 M.-Z. Wang,<sup>23</sup> Y. Watanabe,<sup>43</sup> E. Won,<sup>14</sup> Q. L. Xie,<sup>9</sup> B. D. Yabsley,<sup>47</sup> A. Yamaguchi,<sup>41</sup> Y. Yamashita,<sup>25</sup>  
 M. Yamauchi,<sup>7</sup> J. Ying,<sup>31</sup> S. L. Zang,<sup>9</sup> C. C. Zhang,<sup>9</sup> J. Zhang,<sup>7</sup> L. M. Zhang,<sup>33</sup> Z. P. Zhang,<sup>33</sup> and V. Zhilich<sup>1</sup>

(The Belle Collaboration)

<sup>1</sup>*Budker Institute of Nuclear Physics, Novosibirsk*

<sup>2</sup>*Chiba University, Chiba*

<sup>3</sup>*Chonnam National University, Kwangju*

<sup>4</sup>*University of Cincinnati, Cincinnati, Ohio 45221*

<sup>5</sup>*University of Frankfurt, Frankfurt*

<sup>6</sup>*University of Hawaii, Honolulu, Hawaii 96822*

<sup>7</sup>*High Energy Accelerator Research Organization (KEK), Tsukuba*

<sup>8</sup>*Hiroshima Institute of Technology, Hiroshima*

<sup>9</sup>*Institute of High Energy Physics, Chinese Academy of Sciences, Beijing*

<sup>10</sup>*Institute of High Energy Physics, Vienna*

<sup>11</sup>*Institute for Theoretical and Experimental Physics, Moscow*

<sup>12</sup>*J. Stefan Institute, Ljubljana*

<sup>13</sup>*Kanagawa University, Yokohama*

<sup>14</sup>*Korea University, Seoul*

<sup>15</sup>*Swiss Federal Institute of Technology of Lausanne, EPFL, Lausanne*

<sup>16</sup>*University of Ljubljana, Ljubljana*

<sup>17</sup>*University of Maribor, Maribor*

<sup>18</sup>*University of Melbourne, Victoria*

<sup>19</sup>*Nagoya University, Nagoya*

<sup>20</sup>*Nara Women's University, Nara*

<sup>21</sup>*National Central University, Chung-li*

<sup>22</sup>*National United University, Miao Li*

<sup>23</sup>*Department of Physics, National Taiwan University, Taipei*

<sup>24</sup>*H. Niewodniczanski Institute of Nuclear Physics, Krakow*

<sup>25</sup>*Nippon Dental University, Niigata*

<sup>26</sup>*Niigata University, Niigata*

<sup>27</sup>*Nova Gorica Polytechnic, Nova Gorica*

<sup>28</sup>*Osaka City University, Osaka*

<sup>29</sup>*Osaka University, Osaka*

<sup>30</sup>*Panjab University, Chandigarh*

<sup>31</sup>*Peking University, Beijing*

<sup>32</sup>*Princeton University, Princeton, New Jersey 08544*

<sup>33</sup>*University of Science and Technology of China, Hefei*

<sup>34</sup>*Seoul National University, Seoul*

<sup>35</sup>*Shinshu University, Nagano*

<sup>36</sup>*Sungkyunkwan University, Suwon*

<sup>37</sup>*University of Sydney, Sydney NSW*

<sup>38</sup>*Tata Institute of Fundamental Research, Bombay*

<sup>39</sup>*Toho University, Funabashi*

<sup>40</sup>*Tohoku Gakuin University, Tagajo*

<sup>41</sup>*Tohoku University, Sendai*

<sup>42</sup>*Department of Physics, University of Tokyo, Tokyo*

<sup>43</sup>*Tokyo Institute of Technology, Tokyo*

<sup>44</sup>*Tokyo Metropolitan University, Tokyo*

<sup>45</sup>*Tokyo University of Agriculture and Technology, Tokyo*

<sup>46</sup>*University of Tsukuba, Tsukuba*

<sup>47</sup>*Virginia Polytechnic Institute and State University, Blacksburg, Virginia 24061*

<sup>48</sup>*Yonsei University, Seoul*

(Dated: August 23, 2019)

A search for mixing in the neutral  $D$  meson system has been performed using semileptonic  $D^0 \rightarrow K^{(*)-} e^+ \nu$  decays. Neutral  $D$  mesons from  $D^{*+} \rightarrow D^0 \pi^+$  decays are used; the flavor at production is tagged by the charge of the slow pion. The measurement is performed using  $253 \text{ fb}^{-1}$  of data recorded by the Belle detector. From the yield of right-sign and wrong-sign decays arising from non-mixed and mixed events, respectively, we estimate the upper limit of the time-integrated mixing rate to be  $r_D < 1.0 \times 10^{-3}$  at 90% C.L.

PACS numbers: 14.40.Lb, 13.20.Fc, 12.15.Ff, 11.30.Er

## I. INTRODUCTION

The phenomenon of mixing has been observed in the  $K^0 - \bar{K}^0$  and  $B^0 - \bar{B}^0$  systems, but not yet in the  $D^0 - \bar{D}^0$  system. The parameters used to characterize  $D^0 - \bar{D}^0$  mixing are  $x = \Delta m / \bar{\Gamma}$  and  $y = \Delta \Gamma / 2\bar{\Gamma}$ , where  $\Delta m$  and  $\Delta \Gamma$  are the differences in mass and decay width between the two neutral charmed meson mass eigenstates, and  $\bar{\Gamma}$  is the mean decay width. The mixing rate within the Standard Model is expected to be small [1]: the largest predicted values, including the impact of long distance dynamics, are of order  $x \lesssim y \sim 10^{-3} - 10^{-2}$ . Observation of a mixing rate significantly larger than predicted would indicate either new physics (enhanced  $x$ ) or insufficient understanding of long distance effects (larger  $y$ ).

For  $x, y \ll 1$  and negligible CP violation, the time-dependent mixing probability for semileptonic  $D^0$  decays is [2]

$$\mathcal{P}(D^0 \rightarrow \bar{D}^0 \rightarrow X^+ \ell^- \bar{\nu}_\ell) \propto r_D t^2 e^{-\Gamma t}, \quad (1)$$

where  $r_D$  is the ratio of the time-integrated mixing to the time-integrated non-mixing probability:

$$r_D = \frac{\int_0^\infty dt \mathcal{P}(D^0 \rightarrow \bar{D}^0 \rightarrow X^+ \ell^- \bar{\nu}_\ell)}{\int_0^\infty dt \mathcal{P}(D^0 \rightarrow X^- \ell^+ \nu_\ell)} \approx \frac{x^2 + y^2}{2}. \quad (2)$$

In this paper we present a search for  $D^0 - \bar{D}^0$  mixing using semileptonic decays of charmed mesons. The flavor of a neutral  $D$  meson at production is determined from the charge of the accompanying slow pion ( $\pi_s$ ) in the  $D^{*+} \rightarrow D^0 \pi_s^+$  decay [3]. We reconstruct the  $D^0$  as  $D^0 \rightarrow K^{(*)-} e^+ \nu_e$  and identify its flavor at the time of decay from the charge correlation of the kaon and the electron. We search for mixing by reconstructing the “wrong

sign” (WS) decay chain,  $D^{*+} \rightarrow D^0 \pi_s^+$ ,  $D^0 \rightarrow \bar{D}^0$ ,  $\bar{D}^0 \rightarrow K^{(*)+} e^- \bar{\nu}_e$ , which results in a WS charge combination of the three particles used to reconstruct the candidate. The non-mixed process results in a “right sign” (RS) charge combination,  $\pi_s^+ K^- e^+$ . In contrast to hadronic decays, the WS charge combinations can occur only through mixing, and  $r_D$  can be obtained directly as the ratio of WS to RS signal events.

We make no attempt to reconstruct  $K^{*-}$  mesons. We treat charged daughter particles ( $K^-$  or  $\pi^-$ ) as if they were the direct daughters of the  $D^0$ , omitting the accompanying neutral particle. A small contribution from  $D^0 \rightarrow \rho^- e^+ \nu_e$  and  $D^0 \rightarrow \pi^- e^+ \nu_e$  decays, due to charged pions surviving the kaon selection, is included in the analysis.

We measure  $r_D$  in a  $253 \text{ fb}^{-1}$  data sample recorded by the Belle detector at the KEKB asymmetric-energy  $e^+ e^-$  collider [4], at a center-of-mass (cms) energy of about 10.6 GeV. The Belle detector [5] is a large-solid-angle magnetic spectrometer that consists of a silicon vertex detector (SVD), a 50-layer central drift chamber (CDC), an array of aerogel threshold Čerenkov counters (ACC), a barrel-like arrangement of time-of-flight scintillation counters (TOF), and an electromagnetic calorimeter (ECL) comprised of CsI(Tl) crystals located inside a superconducting solenoid coil that provides a 1.5 T magnetic field. An iron flux-return located outside of the coil is instrumented to detect  $K_L^0$  mesons and to identify muons (KLM). Two different inner detector configurations were used. The first  $140 \text{ fb}^{-1}$  of data were taken using a 2.0 cm radius beampipe and a 3-layer silicon vertex detector, and the subsequent  $113 \text{ fb}^{-1}$  were taken using a 1.5 cm radius beampipe, a 4-layer silicon detector and a small-cell inner drift chamber [6].

Simulated events are generated by the QQ generator and processed with a full simulation of the Belle detector, using the GEANT package [7]. To simulate mixed  $D$  meson decays we use generic (non-mixed) Monte Carlo (MC) events and appropriately reweight the proper decay time distribution.

## II. SELECTION AND RECONSTRUCTION

For  $\pi_s^+$  candidates we consider tracks with: momentum  $p < 600 \text{ MeV}/c$ ; projections of the impact parameter with respect to the interaction point in the radial and beam directions  $dr < 1 \text{ cm}$  and  $|dz| < 2 \text{ cm}$ , respectively; and electron identification likelihood ratio, based on the information from the CDC, ACC and ECL [8],  $\mathcal{L}_e < 0.1$ . Electron candidates are required to have  $p > 600 \text{ MeV}/c$  and  $\mathcal{L}_e > 0.95$ . Kaon candidates are chosen from the remaining tracks in the event with  $p > 800 \text{ MeV}/c$  and  $\mathcal{L}(K^\pm)/(\mathcal{L}(K^\pm) + \mathcal{L}(\pi^\pm)) > 0.5$ , where  $\mathcal{L}(K^\pm, \pi^\pm)$  is the likelihood that a given track is a  $K^\pm$  or a  $\pi^\pm$  based on information from the TOF, CDC and ACC. Charged pions originating from semileptonic  $D^0 \rightarrow \pi^- e^+ \nu_e$  decays that pass the kaon selection criteria are treated as kaons and assigned the kaon mass. According to MC simulation, this selection retains about 58% (43%, 52%) of signal slow pions (electrons, kaons), and at this stage about 13% (5%, 44%) of the selected  $\pi_s$  ( $e$ ,  $K$ ) candidates are misidentified.

The variable used to isolate the signal events is  $\Delta M = M(\pi_s K e \nu_e) - M(K e \nu_e)$ , where  $M(\pi_s K e \nu_e)$  and  $M(K e \nu_e)$  are the invariant masses of the selected charged particles and reconstructed neutrino (see below), with and without the slow pion.

We require the cms momentum of the kaon-electron system to be  $p_{\text{cms}}(Ke) > 2 \text{ GeV}/c$  to reduce the combinatorial background and the background from  $B\bar{B}$  events, and to improve the resolution in  $\Delta M$ . To further suppress the contribution of  $B\bar{B}$  events, we require the ratio of the second to the zeroth Fox-Wolfram moments, known as  $R_2$ , to be greater than 0.2 [9].

Background from  $D^0 \rightarrow K^- \pi^+$  decay is suppressed by requiring the invariant mass of the  $K$ - $e$  system to satisfy  $M(Ke) < 1.82 \text{ GeV}/c^2$ . Background from  $D^0 \rightarrow K^- K^+$  decay is effectively reduced by the requirement  $|M(KK) - m_{D^0}| > 10 \text{ MeV}/c^2$ , where  $M(KK)$  is the  $K$ - $e$  invariant mass, calculated using the kaon mass for both tracks.

The background from photon conversions, where the  $e^-$  and  $e^+$  are taken to be the electron and slow pion candidates, is suppressed by requiring  $M(e^+e^-) > 150 \text{ MeV}/c^2$ , where  $M(e^+e^-)$  is the invariant mass of the  $\pi_s^+ e^-$  system with the electron mass assigned to the pion. A further search for an additional  $e^\pm$  with charge opposite to that of the electron (slow pion) candidate in the  $D^0$  ( $D^{*+}$ ) decay is performed in each event.

Again, candidates with  $M(e^+e^-)$  below  $150 \text{ MeV}/c^2$  are rejected.

The first approximation to the neutrino four-momentum is calculated from four-momentum conservation:

$$P_\nu = P_{\text{cms}} - P_{\pi_s K e} - P_{\text{rest}}, \quad (3)$$

where  $P_{\text{cms}}$  denotes the cms four-momentum of the  $e^+e^-$  system,  $P_{\pi_s K e}$  the cms four-momentum of the  $\pi_s$ - $K$ - $e$  combination, and  $P_{\text{rest}}$  the cms four-momenta of all remaining charged tracks and photons in the event. The  $\Delta M$  resolution is significantly improved by applying two kinematic constraints to correct  $P_{\text{rest}}$ . First, events with  $-4 \text{ GeV}^2/c^4 < M(\pi_s K e \nu)^2 < 36 \text{ GeV}^2/c^4$  are selected and the magnitude of  $P_{\text{rest}}$  is rescaled by a factor  $x$  such that  $M(\pi_s K e \nu)^2 = (P_{\text{cms}} - x P_{\text{rest}})^2 \equiv m_{D^{*\pm}}^2$ , with  $m_{D^{*\pm}}$  fixed to its nominal value [10]. Next, only events with  $-2 \text{ GeV}^2/c^4 < M_\nu^2 < 0.5 \text{ GeV}^2/c^4$  are retained and the direction of the three-momentum  $\vec{p}_{\text{rest}}$  is corrected in order to yield  $M_\nu^2 \equiv 0$ . The correction rotates  $\vec{p}_{\text{rest}}$  in the plane determined by the vectors  $\vec{p}_{\text{rest}}$  and  $\vec{p}_{\pi_s K e}$ .

The mass difference  $\Delta M$  is then calculated using this reconstructed neutrino four-momentum. The full width at half maximum (FWHM) of the  $\Delta M$  peak in MC simulated  $D^0 \rightarrow K^- e^+ \nu$  events is found to be  $7 \text{ MeV}/c^2$ . Events with  $\Delta M < 0.18 \text{ GeV}/c^2$  are retained for further analysis.

According to MC simulation, the  $D^0 \rightarrow K^{*-} e^+ \nu_e$ ,  $\rho^- e^+ \nu_e$ , and  $\pi^- e^+ \nu_e$  modes have  $\Delta M$  distributions similar to that from  $D^0 \rightarrow K^- e^+ \nu_e$  decay, but with a larger FWHM. The charge correlation is preserved if the slow pion decays into a muon, and the muon is taken as the slow pion candidate. These decays will be referred to as ‘‘associated signal’’ decays. Their fraction in the reconstructed MC signal sample is  $14.9 \pm 0.1\%$ , with the quoted error being due to MC statistics only.

According to MC, the backgrounds for both RS and WS decays consist mainly of combinatorial background (98.4% and 98.0%, respectively). In order to minimize systematic uncertainties, we model the shape of this background using data, following a method validated with MC events. We use candidates with the unphysical sign combinations  $\pi_s^+ K^- e^-$  and  $\pi_s^+ K^+ e^+$  to model the combinatorial background in the RS sample. In the WS sample this background is mainly due to random  $\pi_s^+$  candidates combined with the selected kaon and electron candidates, and is modelled by combining  $\pi_s^+$  and  $(K^- + e^+)$  candidates from different events. The correlated background (1.6% in the RS, 2.0% in the WS sample) arises from a true  $\pi_s^+$  from a  $D^{*+}$  decay combined with true or misidentified  $K$  and  $e$  candidates, both (in the RS sample) or at least one of them (WS sample) from the corresponding  $D^0$  decay. This background is described using MC.

Figure 1 shows the  $\Delta M$  distribution for RS events. We perform a binned maximum likelihood fit to the distri-

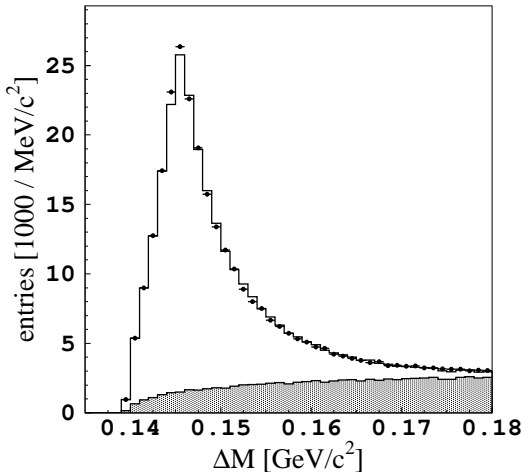


FIG. 1:  $\Delta M$  distribution for RS events. The data (background) is represented by points (hatched histogram), and the result of the binned maximum likelihood fit by the solid line.

bution, maximizing

$$\mathcal{L} = \prod_{i=1}^{N_{\text{bin}}} \frac{e^{-\mu(\Delta M_i)} \times (\mu(\Delta M_i))^{N_i}}{N_i!}, \quad (4)$$

where  $N_i$  is the number of entries in the  $i$ -th bin and  $\mu(\Delta M_i)$  is the expected number of events in this bin, given by

$$\mu(\Delta M_i) = \mathcal{N}[f_s P_s(\Delta M_i) + (1 - f_s) P_b(\Delta M_i)]. \quad (5)$$

$P_s$  ( $P_b$ ) is the signal (background)  $\Delta M$  distribution obtained from MC (as described above);  $f_s$  and  $\mathcal{N}$  are the signal fraction and the overall normalization, respectively, and are free parameters in the fit. The hatched histogram in Fig. 1 shows the fitted background contribution. The fitted signal fraction is  $f_s = 73.4 \pm 0.1\%$  and the number of RS signal events is  $N_{\text{RS}}^{\text{tot}} = 229\,452 \pm 597$ .

We increase the sensitivity to  $D^0 - \bar{D}^0$  mixing by exploiting the measurement of the  $D^0$  proper decay time. The decay time is evaluated using the measured momentum of the meson and the distance from the  $e^+e^-$  interaction point to the reconstructed  $D^0$  decay  $K$ - $e$  vertex. Due to the shape of the KEKB accelerator interaction region, which is narrowest in the vertical ( $y$ ) direction, the dimensionless proper decay time  $t_y$  is calculated as

$$t_y = \frac{m_{D^0}}{c\tau_{D^0}} \frac{y_{\text{vtx}} - y_{\text{IP}}}{p_y}, \quad (6)$$

where  $p_y$  is the  $y$  component of the  $D^0$  candidate's momentum and  $y_{\text{vtx}}$  and  $y_{\text{IP}}$  are the  $y$  coordinates of the reconstructed  $K$ - $e$  vertex and of the interaction point, respectively.  $m_{D^0}$  and  $\tau_{D^0}$  are the nominal mass and lifetime of  $D^0$  mesons [10].

Mixed and non-mixed processes have different proper decay time distributions:  $t^2 e^{-t/\tau_{D^0}}$  and  $e^{-t/\tau_{D^0}}$ , respectively. In order to calculate the mixing parameter  $r_D$  after any selection based on  $D^0$  proper decay time, the ratio of the two types of signal events,  $N_{\text{WS}}/N_{\text{RS}}$ , must be multiplied by the ratio of their efficiencies,  $\epsilon_{\text{RS}}/\epsilon_{\text{WS}}$ . The efficiencies are obtained by integrating the convolution of the above proper decay time distributions with the detector resolution function, over the selected  $t_y$  interval. As the observed proper decay time distribution is a convolution of the signal and background probability density functions (p.d.f.) with the detector resolution function, the latter is found by performing a binned  $\chi^2$  fit to the RS event  $t_y$  distribution:  $\int_0^\infty dt [f_s e^{-t/\tau_{D^0}} + (1 - f_s)(f_e e^{-t/\tau_{\text{bkg}}} + (1 - f_e)\delta(t))] \times \mathcal{R}(t/\tau_{D^0} - t_y)$ . The signal fraction  $f_s$  is obtained from the fit to the  $\Delta M$  distribution. The fraction  $f_e$  of the non-prompt background component and its lifetime  $\tau_{\text{bkg}}$  are fixed to the values obtained by fitting the MC background  $t_y$  distributions;  $\delta(t)$  describes the shape of the prompt background component. The resolution function  $\mathcal{R}(t - t_y)$  is described phenomenologically by the sum of three Gaussians and an additional term for badly reconstructed tracks (“outliers”); we obtain the widths and coefficients from the fit.

The ratios  $\epsilon_{\text{RS}}/\epsilon_{\text{WS}}$  are given in Table I. The errors are obtained by varying each parameter in the proper decay time fit by  $\pm 1\sigma$ , repeating the fit and recalculating the ratios; the resulting changes are summed in quadrature. Using this method, the majority of systematic errors due to the imperfect description of the decay time distribution cancel out.

Comparison of the expected  $t_y$  distribution for WS signal and background events indicates that the figure-of-merit, defined as  $N_{\text{WS}}^{\text{sig}}/\sqrt{N_{\text{WS}}^{\text{bkg}}}$ , is optimal for  $t_y \geq 1.0$ . Events that satisfy this condition are retained for further analysis.

### III. FIT AND RESULTS

We extract the RS and WS signal yields separately in six intervals of  $t_y$ . The yields are obtained from binned maximum likelihood fits to  $\Delta M$ , described by Eq. 4; the WS signal distribution is taken to be the same as the RS. The results are shown in Table I and Fig. 2. We obtain the time-integrated mixing probability ratio in the  $i$ -th  $t_y$  interval,  $r_D^i = N_{\text{WS}}^i/N_{\text{RS}}^i \times \epsilon_{\text{RS}}^i/\epsilon_{\text{WS}}^i$ , by multiplying the ratio of WS to RS signal events in each interval by the  $t_y$  efficiency ratio. The mixing probability is compatible with zero in all proper decay time intervals (see Fig. 3).

The overall  $r_D$  follows from a  $\chi^2$  fit with a constant to the measured  $r_D^i$  values, using a constant:

$$r_D = (0.20 \pm 0.47) \times 10^{-3}. \quad (7)$$

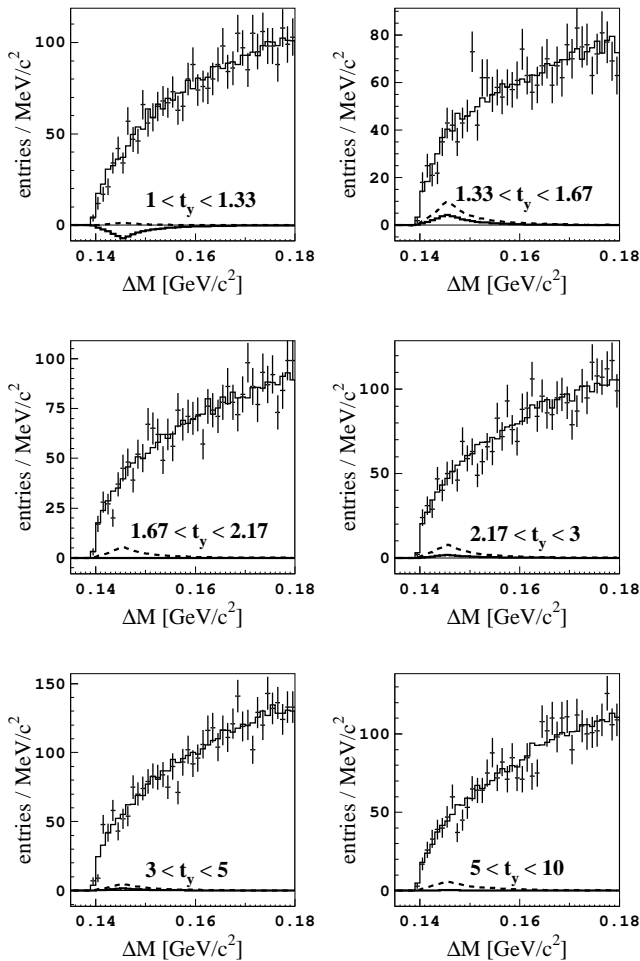


FIG. 2: WS  $\Delta M$  distributions in six proper decay time intervals for data (points with error bars) and the results of the fit described in the text (solid line). At the bottom of each figure the fitted (expected for  $r_D^i = 90\%$  C.L. upper limit) signal yield is plotted as a solid (dashed) line.

The quoted error is statistical only.

#### IV. SYSTEMATIC UNCERTAINTIES

The experimental procedure was checked using a dedicated MC sample of mixed  $D^0$  decays. These were added in different proportions to the generic MC, which includes both non-mixed  $D^0$  decays and all known types of background decays. The application of the same method used for the data on these samples verified that the reconstructed  $r_D$  value reproduces the input value without any significant bias.

The main source of systematic error is the limited statistics of the fitting distributions, predominantly the background distribution in the WS sample. To estimate

TABLE I: The number of fitted signal events in the RS and WS samples, the efficiency ratio  $\epsilon_{\text{RS}}^i/\epsilon_{\text{WS}}^i$ , and the resulting  $r_D^i$  value for each proper decay time interval.

$t_y$	$N_{\text{RS}}^i$	$N_{\text{WS}}^i$	$\epsilon_{\text{RS}}^i/\epsilon_{\text{WS}}^i$	$r_D^i [10^{-3}]$
1.00-1.33	$18\,742 \pm 166$	$-63.7 \pm 30.2$	$1.62 \pm 0.11$	$-5.49 \pm 2.63$
1.33-1.67	$15\,032 \pm 147$	$40.3 \pm 29.9$	$1.14 \pm 0.08$	$3.05 \pm 2.27$
1.67-2.17	$16\,430 \pm 155$	$-1.3 \pm 30.6$	$0.79 \pm 0.05$	$-0.06 \pm 1.48$
2.17-3.00	$16\,691 \pm 157$	$17.0 \pm 33.1$	$0.51 \pm 0.03$	$0.51 \pm 1.00$
3.00-5.00	$15\,443 \pm 160$	$14.7 \pm 37.4$	$0.30 \pm 0.01$	$0.28 \pm 0.72$
5.00-10.0	$8\,263 \pm 123$	$3.0 \pm 35.2$	$0.28 \pm 0.02$	$0.10 \pm 1.19$

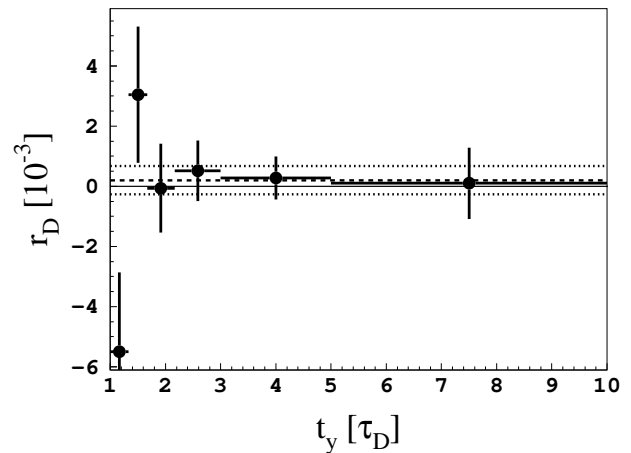


FIG. 3: Measured  $r_D^i$  values (points with error bars) in six different proper decay time intervals. The solid (dashed) line shows the null value (the fit to the six  $r_D^i$  using a constant). The dotted lines denote the statistical error of the fit.

this uncertainty, we vary the contents of all bins of the RS and WS  $P_s(\Delta M)$  and  $P_b(\Delta M)$  distributions independently in accordance with each bin's statistical uncertainty, repeat the fit to the RS and WS data, calculate the corresponding  $r_D^i$  in each proper decay time interval, and obtain a new  $r_D$  value. Repeating the procedure, the obtained distribution of  $r_D$  values has a Gaussian shape with a width of  $0.12 \times 10^{-3}$ , which is taken as the systematic error due to the limited statistics of the fitting distributions.

To estimate the systematic uncertainty due to the  $\Delta M$  binning and the shape of the WS background, the  $\Delta M$  distributions in each proper decay time interval, originally divided into 45 bins in the range  $0.135 \text{ GeV}/c^2 < \Delta M < 0.180 \text{ GeV}/c^2$ , are re-binned into 12, 15, 20, 30 and 60 bins in the same range. The fitting procedure is repeated for each set of bins, and the systematic error due to binning is taken as half the difference between the largest and the smallest  $r_D$ :  $\pm 0.07 \times 10^{-3}$ .

According to MC, the majority of the correlated WS background arises from  $D^0 \rightarrow K^-\pi^+\pi^0$  decays. We repeat the WS fits, changing the amount of this background in accordance with the relative error on  $\mathcal{B}(D^0 \rightarrow$

$K^-\pi^+\pi^0$ ). The resulting variation in  $r_D$  is  $\pm 0.02 \times 10^{-3}$ . The same method applied in the fit to the RS sample introduces a negligible variation of the  $r_D$  value (less than  $0.001 \times 10^{-3}$ ).

We compare the  $\epsilon_{\text{RS}}^i$  values with the corresponding  $N_{\text{RS}}^i/N_{\text{RS}}^{\text{tot}}$  ratios. The relative difference between the two is conservatively assigned as the uncertainty on  $\epsilon_{\text{RS}}^i/\epsilon_{\text{WS}}^i$ , although one expects at least part of the systematic uncertainty to cancel in the efficiency ratio. We reduce the six efficiency ratios simultaneously by this uncertainty and repeat the  $r_D$  calculation; we then increase the ratios by this uncertainty, and again recalculate  $r_D$ . We quote the difference between the resulting  $r_D$  values and the default fit ( $\pm 0.02 \times 10^{-3}$ ) as the systematic error due to an imperfect description of the proper decay time distributions.

The systematic error due to the uncertainty in the associated signal fraction is estimated by varying the fraction and repeating the fitting procedure. Using the errors on the measured branching fractions [10] of the associated signal decay channels, we conservatively vary the amount of associated signal by  $\pm 40\%$ . We recalculate  $r_D$  and compare it to the default  $r_D$  value; we quote the difference,  $0.002 \times 10^{-3}$ , as the systematic error from this source.

The quadratic sum of these individual contributions yields a total systematic error of  $\pm 0.14 \times 10^{-3}$ .

## V. CONCLUSION

In summary, we have searched for  $D^0 - \bar{D}^0$  mixing in semileptonic  $D^0$  decays. We independently measure the mixing ratios  $r_D^i$  in six  $D^0$  proper decay time intervals. By fitting a constant to these six values we obtain the final result

$$r_D = (0.20 \pm 0.47 \pm 0.14) \times 10^{-3}, \quad (8)$$

where the first error is the statistical and the second the systematic uncertainty. As we do not observe a significant number of WS  $D^0$  decays, we obtain an upper limit for the time-integrated mixing rate. We use the Feldman-Cousins approach [11] to calculate the upper limit in the vicinity of the physics region boundary ( $r_D \geq 0$ ). Using the result and the total error in Eq. 8, this yields

$$r_D \leq 1.0 \times 10^{-3} \quad \text{at 90\% C.L.} \quad (9)$$

This result is the most stringent experimental limit on the time-integrated  $D^0$  mixing rate obtained to date from semileptonic  $D^0$  decays [10].

## ACKNOWLEDGMENTS

We thank the KEKB group for the excellent operation of the accelerator, the KEK cryogenics group for the efficient operation of the solenoid, and the KEK computer group and the NII for valuable computing and Super-SINET network support. We acknowledge support from MEXT and JSPS (Japan); ARC and DEST (Australia); NSFC (contract No. 10175071, China); DST (India); the BK21 program of MOEHRD, and the CHEP SRC and BR (grant No. R01-2005-000-10089-0) programs of KOSEF (Korea); KBN (contract No. 2P03B 01324, Poland); MIST (Russia); MHEST (Slovenia); SNSF (Switzerland); NSC and MOE (Taiwan); and DOE (USA).

- 
- [1] For a review see for example S. Bianco, F.L. Fabbri, D. Benson and I. Bigi, Riv. Nuovo Cim. **26N7**, 1 (2003); also A. Falk *et al.*, Phys. Rev D **69**, 114021 (2004).
  - [2] Z.-Z. Xing, Phys. Rev. D **55**, 196 (1997).
  - [3] Charge-conjugate modes are implied throughout this paper.
  - [4] S. Kurokawa and E. Kikutani, Nucl. Instr. Meth. A **499**, 1 (2003), and other papers included in this volume.
  - [5] A. Abashian *et al.* (Belle), Nucl. Instr. Meth. A **479**, 117 (2002).
  - [6] Y. Ushiroda *et al.*, Nucl. Instr. Meth. A **511**, 6 (2003).
  - [7] Events are generated with the CLEO QQ generator (see <http://www.lns.cornell.edu/public/CLEO/soft/qq/>); the detector response is simulated with GEANT, R. Brun *et al.*, GEANT 3.21, CERN Report DD/EE/84-1, (1984).
  - [8] K. Hanagaki *et al.*, Nucl. Instrum. Meth. A **485**, 490 (2002).
  - [9] G.C. Fox and S. Wolfram, Phys. Rev. Lett. **41**, 1581 (1978).
  - [10] S. Eidelman *et al.*, Phys. Lett. B **592**, 1 (2004).
  - [11] G.J. Feldman and R.D. Cousins, Phys. Rev. D **57**, 3873 (1998).